Analysis of Cogging Torque in Interior Permanent Magnet Motor by Analytical Method

Gyu-Hong Kang, Jung-Pyo Hong and Gyu-Tak Kim

Abstract - This paper deals with magnetic field analysis and computation of cogging torque using an analytical method in Interior Permanent Magnet Motor (IPMM). The magnetic field is analyzed by solving space harmonics field analysis due to magnetizing distribution and the cogging torque is analyzed by combining field analysis with relative permeance. In reducing cogging torque, the inferences of various design variable and magnetizing distribution are investigated. It is shown that the slot and pole ratio (the pole-arc / pole-pitch ratio) combination has a significant effect on the cogging torque and presents a optimal flux barrier shape to reduce the cogging torque. The validity of the proposed technique is confirmed with 2-D Finite Element(FE) analysis.

Key Words - Interior Permanent Magnet Motor(IPMM), space harmonics field analysis, relative permeance, 2-D Finite Element(FE).

1. Introduction

Permanent Magnet (PM) motors have been used in a wide variety of speed control application. In Interior Permanent Magnet Motor (IPMM) used for variable-speed drives, the separation of PM caused by the centrifugal force at high speed can be avoided since the PM is inserted into the rotor core [1]. The IPMM generates the reluctance torque due to saliency of the rotor. Due to this nature, IPMM is studied by many researchers recently.

The components of cogging torque that produces both vibration and noise are due to the interaction between PMs and the air-gap permeance harmonics. The IPMM has some advantages, such as high torque and power density, to reduce the magnet requirements. On the other hand, the IPMM has significant cogging torque due to the unique IPMM structure and the identical sizes of effective and mechanical airgap. The field and cogging torque characteristics are quite sensitive to the geometry of the rotor and the stator due to the small air-gap [2]. For this reason, it is necessary to have numerical methods which can consider geometric details and the non-linearity of magnetic material. To improve the accuracy in the computation, it is usual to take significantly long time for the optimization of many design parameters [3-4].

In this paper, we develop the analytical method to calculate magnetic field and cogging torque of IPMM [5]. In the case of IPMM, the actual pole ratio is different to the effective pole ratio. The difference is due to the leakage and fringing effect in link part that is working for flux barrier. To overcome the problem, this paper presents analysis method to account equivalent magnetizing distribution in accordance with leakage and fringing effect in flux barrier. By using the analytical method, the rotor shape to reduce the cogging torque under the constant magnet dimension without skewing can be proposed. The results of the proposed analysis and the design of the rotor shape are verified by comparing with the 2-D Finite Element (FE) analysis.

Manuscript received: Feb. 6, 2001 accepted: Apr. 18, 2001.

Gyu-Hong Kang, Jung-Pyo Hong, Gyu-Tak Kim are with the Department of Electrical Engineering, Changwon National University, 9 Sarim-dong, Changwon-city, kyungnam 641-773, Korea.

2. Magnetic Field Analysis

In this paper, the analytical method to calculate the air-gap flux density distribution and net lateral force acting on the teeth is proposed to predict the cogging torque [4-6].

Fig.1 shows the topologies of IPMM studied in this paper. The IPMM consists of an inserted PM and its stator surface is assumed as smooth. In IPMM, flux dispersion is developing in airgap because the magnet flux passes the iron core and leakage flux in the flux barrier parts. Therefore, the analytical methods require the precise characteristics of magnetization distribution.

The equivalent magnetization with fringing and leakage effects is shown in Fig. 2. The effects of flux dispersion and leakage are considered to increase pole angle and to decrease residual flux density of PM. The area of magnetization is constant.

The magnetization **M** considering fringing and leakage effects represented by a Fourier series expansion is given as follow [3]

$$\vec{M} = M_r \vec{r} = \sum_{n=1,3,5..}^{\infty} M_n \sin(np\theta) \cdot \vec{r} \qquad (1)$$

$$M_n = \frac{-2M_e}{bn^2\pi}\left[\sin an\{1-(-1)^n\} + \sin\{n(a+b)\}\{-1+(-1)^n\}\right]$$

$$\vec{M}(\theta) = \sum_{n=1,3,5..}^{\infty} \frac{-4M_e}{bn^2\pi}\left[\sin(an) - \sin\{n(a+b)\}\right]\sin(np\theta) \tag{2}$$

where, B_r is the residual flux density and p is the pole pair.

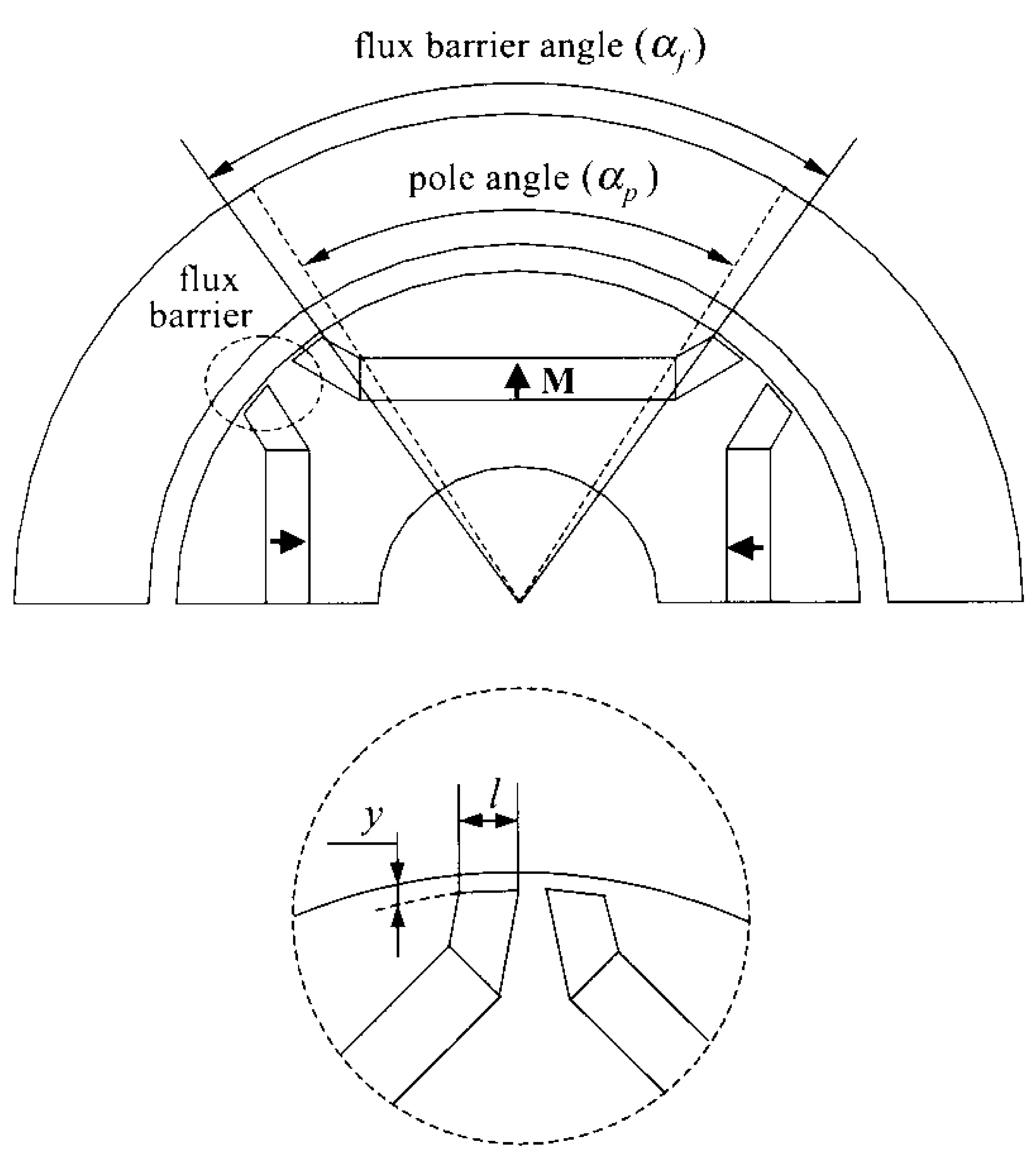

Fig. 1 Motor topology

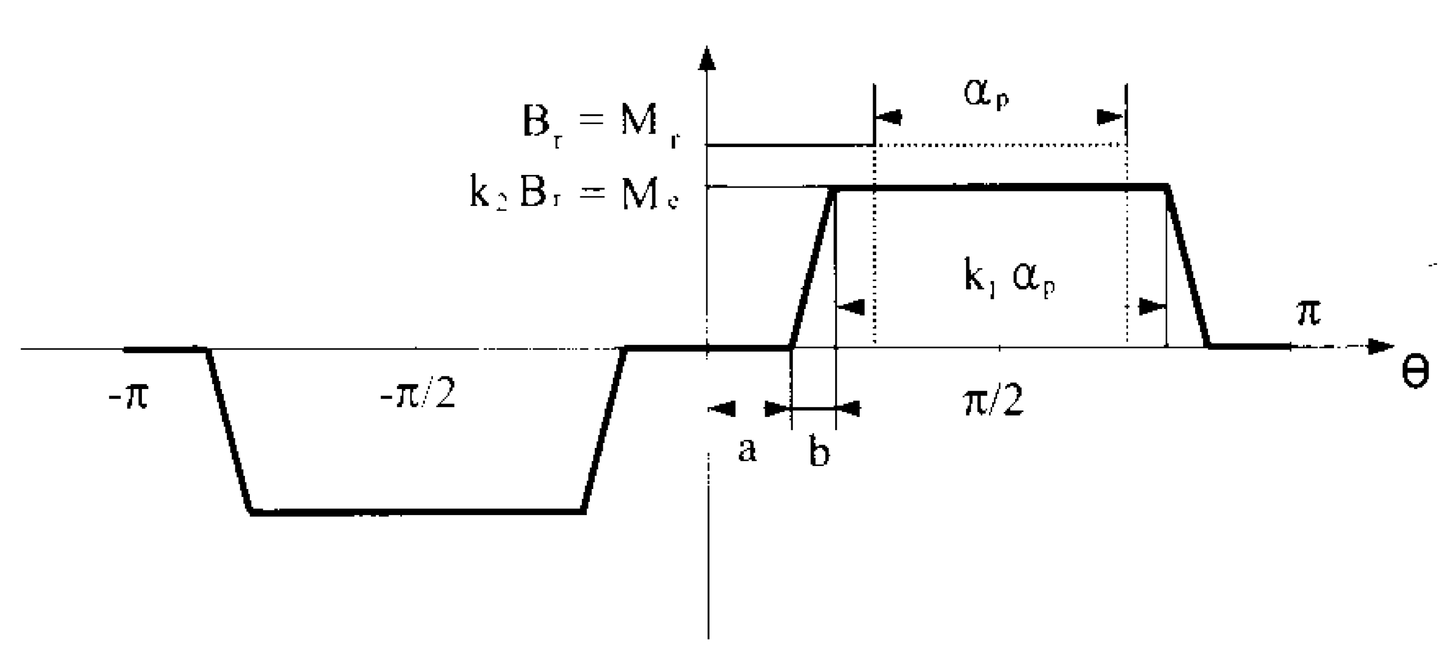

Fig. 2 Magnetizing distribution of IPMM

The flux density in the flux barrier is assumed as entirely saturated to B_s. In this paper, the B_s is set to about 1.8(T) and the coefficients of equivalent magnetization calculation are given by

$$k_1 = \frac{\alpha_f}{\alpha_p} \tag{3}$$

$$k_2 = \frac{1}{k_1}\left(1 - \frac{\psi_l}{\psi_r}\right) \tag{4}$$

$$b = \alpha_p \frac{\psi_l}{\psi_r} \tag{5}$$

where, $\psi_r = B_r \cdot S$, $\psi_l = B_s \cdot y \cdot L$: ψ_r is magnet flux, L is stack length, S is magnet area and ψ_l is leakage flux in flux barrier.

The magnetic field is obtained from equivalent magnetization and the radial component of flux density in air-gap is obtained from Poisson equation [3-4]. The airgap flux density and the flux linkage of phase are given by

$$\frac{\partial^2\varphi}{\partial r^2} + \frac{1}{r}\frac{\partial\varphi}{\partial r} + \frac{1}{r^2}\frac{\partial^2\varphi}{\partial\theta^2} = 0$$

(in the airgap region) (6)

$$\frac{\partial^2\varphi}{\partial r^2} + \frac{1}{r}\frac{\partial\varphi}{\partial r} + \frac{1}{r^2}\frac{\partial^2\varphi}{\partial\theta^2} = \frac{1}{r}\frac{M_r}{\mu_r}$$

(in the magnet region) (7)

$$B_{gr}(r,\theta) = \sum_{n=1,3,5,\cdots}^{\infty} \frac{\mu_0 M_n}{\mu_r}\frac{np}{(np)^2-1}R_r^{-(np-1)} \cdot A \cdot \left[r^{np-1} + R_s^{2np} r^{-(np+1)}\right]\sin(np\theta) \tag{8}$$

$$B_{g\theta}(r,\theta) = \sum_{n=1,3,5,\cdots}^{\infty} \frac{-\mu_0 M_n}{\mu_r}\frac{np}{(np)^2-1}R_r^{-(np-1)} \cdot A \cdot \left[r^{np-1} - R_s^{2np} r^{-(np-1)}\right]\cos(np\theta) \tag{9}$$

$$R_m = R_r - h_m \tag{10}$$

$$A = \frac{\left[(np-1)R_r^{2np} + 2R_m^{np+1}2R_r^{np-1} - (np+1)R_m^{2np}\right]}{\left[\frac{\mu_r+1}{\mu}\left[R_s^{2np} - R_m^{2np}\right] - \frac{\mu_r-1}{\mu_r}\left[R_r^{2np} - R_s^{2np}(R_m/R_r)^{2np}\right]\right]} \tag{11}$$

where, R_r is radius of rotor including permanent magnet and h_m is magnetizing length of permanent magnet.

From the airgap flux density, the flux linkage of a phase are as follow.

$$\lambda = Nl_s \int_0^{\pi/p} B_{gr}(r,\theta) \cdot r\, d\theta \tag{12}$$

where N is turn number of a phase, l_s is stack length and r is integral path.

3. Computation Method of Cogging Torque

Cogging torque arises from the interaction of the mmf harmonics and the airgap permeance harmonics [5-6]. Therefore an precise analysis technique of airgap field distribution considering slotting effect is required for the calculation of the cogging torque. In this paper, effect of slotting in airgap flux density distribution and characteristic of cogging torque are analyzed by combining relative permeance.

3.1 Magnetic field analysis considering effect of slotting

The magnetic field is obtained from equivalent magnetization and the radial component of flux density in air-gap is obtained from Poisson equation [1].

The calculation of the flux density in the slot-opening region is using relative permeance. It is assumed that the fluxes pass on each side of tooth circularly. The calculation of flux distribution in slot opening region taken into account relative permeance is shown in Fig. 3 [3].

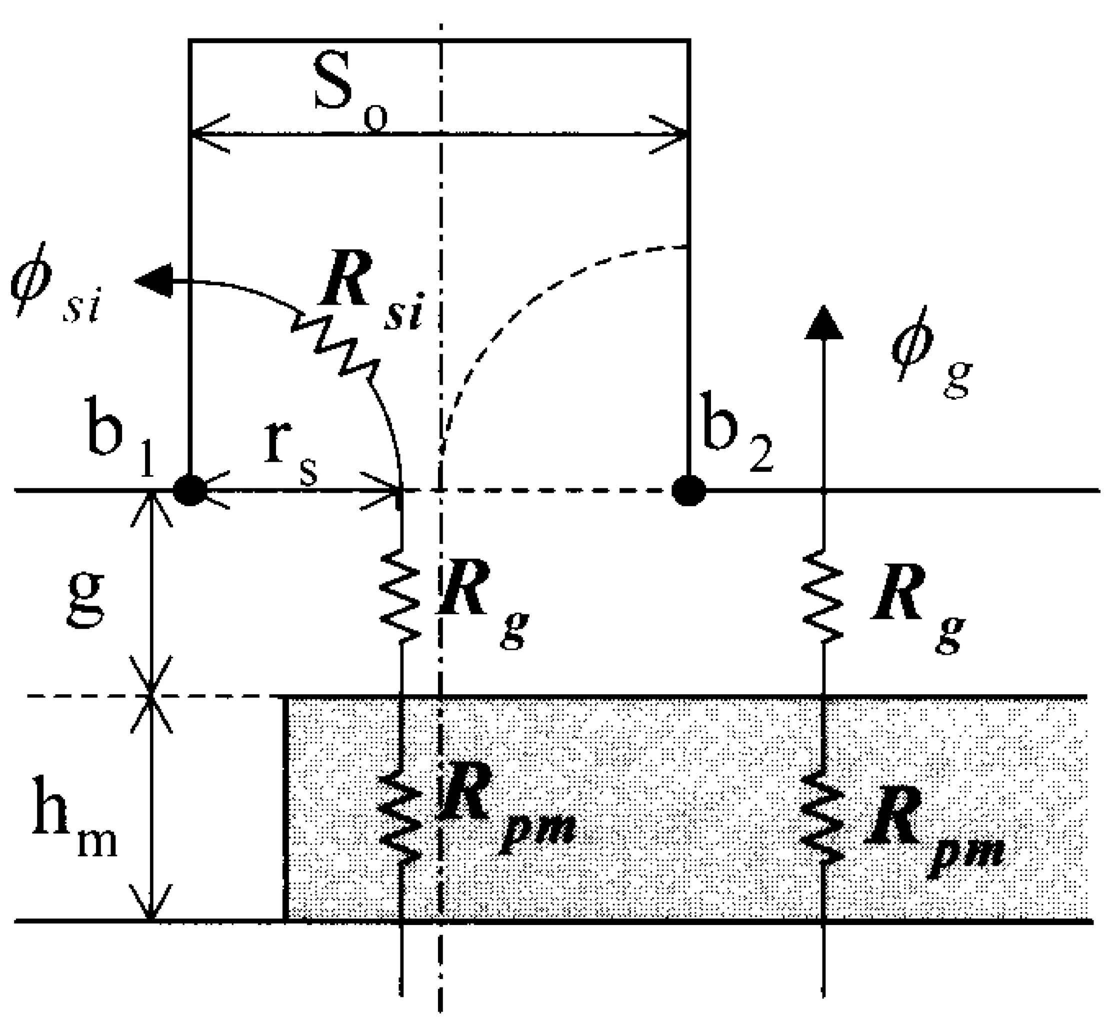

Fig. 3 Computation process of flux density in slots region by relative permeance

The relative permeance $\tilde{P}$ is given by

$$\tilde{P}(x) = \frac{R_{pm} + R_g}{R_{pm} + R_g + R_{si}(x)} \tag{13}$$

$$R_{si}(x) = \frac{r_s}{\mu_0}$$

$$(k-1)\tau_t - \frac{S_0}{2} \le x \le (k-1)\tau_t + \frac{S_0}{2} \tag{14}$$

where, $k = 1, 2, \cdots Q_s$: Q_s is the number of slots, τ_t is the slot pitch and τ_p is the pole pitch.

The flux density of slot opening region is given by

$$B_{si}(x_1) = \tilde{P}(x)\; B_g' \tag{15}$$

The flux density in teeth region is calculated by the reciprocal of relative permeance in order to compensate the reducing of flux density in slot region. The flux density of teeth region is as follows.

$$B_{Ti}(x_1) = \frac{1}{\tilde{P}(x)}\; B_g' \tag{16}$$

3.2 Calculating of cogging torque

For cogging torque calculating, airgap field is analyzed by space harmonics field analysis of magnetization and cogging torque is computed by net lateral force acting on the teeth. In order to calculate cogging torque by analytical method the following assumptions are made :

1) In analysis model, the shape of slots is rectangular
2) the airgap permeance is calculated according to an assumed field pattern in which the flux crosses the airgap straight as shown in Fig. 4.
3) The calculation of the flux density in the slot-opening region is using relative permeance.

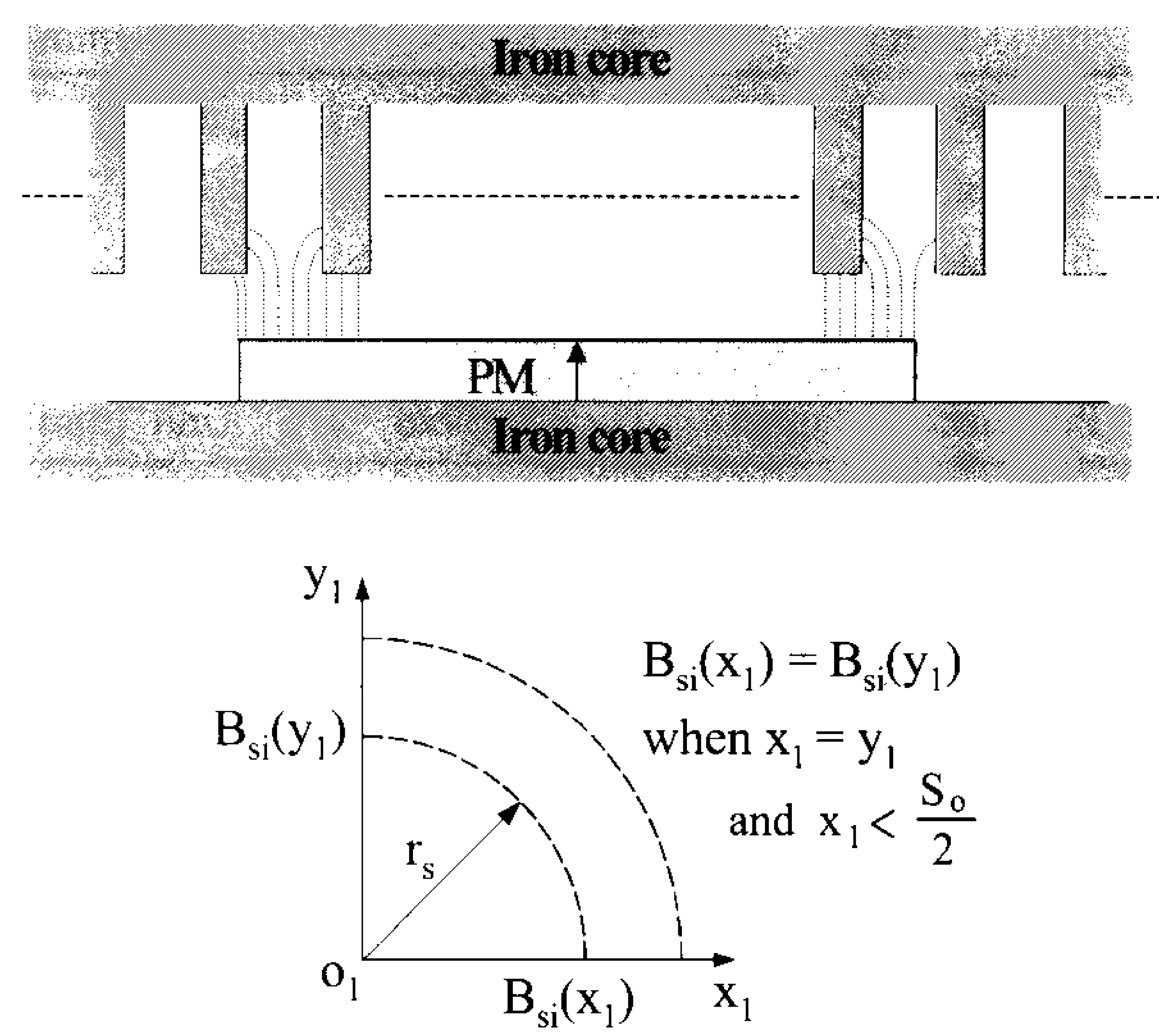

Fig. 4 Assuming flux distribution in slot region

In Fig. 4, S_0 is slot opening width, x_1 is coordinates of slot opening region and y_1 is coordinates of teeth side. The flux in the slot opening region is assumed that the fluxes pass on each side of tooth circularly [5].

The net cogging torque, at any magnet position, is then calculated from flux density in slot-opening region [5-6]. The calculation of flux distribution in slot opening region taken into account relative permeance is shown in Fig. 4. The flux density of slot region and net cogging torque are given by

$$T_c = \sum_{k=1}^{Q_s} l_s \int_0^{S_0/2} \left(\frac{B_{sib_1}^{\,2} - B_{sib_2}^{\,2}}{2\mu_0} \right) \cdot (R_s + r_s)\, dr_s \tag{17}$$

4. Analysis results

The appropriateness of the presented analysis method in IPMM is verified through comparison with 2-D FE analysis. The specification of analysis model is shown in Table 1.

Table 1 Specification of analysis model

Stator	Symbol	Unit [mm]
Inner diameter	D_{si}	91
Slot number	S_T	36
Slot opening width	w_s	5.8
Teeth width	w_t	2.14
Slot depth	h_s	30
Stack length	L_s	87
Airgap	g	2.2
Pole pair	p	2
Rotor	**Symbol**	**Unit [mm]**
Outter diameter	D_{ro}	87
Width of flux barrier	w_l	1
Pole angle	α_p	135°
Flux barrier angle	α_f	148°
Permanent Magnet	**Symbol**	**Unit [mm]**
Residual flux density	B_r	1.12
Width	w_m	47
Magnetizing length	h_m	9

The analysis model has 36 slots, pole angle α_p is 135 (deg. elec.) and flux barrier angle α_f is 148(deg. elec.).

Fig. 5 shows the comparison of the flux density distribution between the proposed analytical method and 2-D FE analysis. In analytical method, it is shown that the slot effect consider by relative permeance and smoothing airgap which is considering carter's coefficient. The characteristics of flux density distribution agree with the 2-D FE analysis, however, the flux density in the flux barrier region and the slot area has a little difference. It is due to saturation degree in the core.

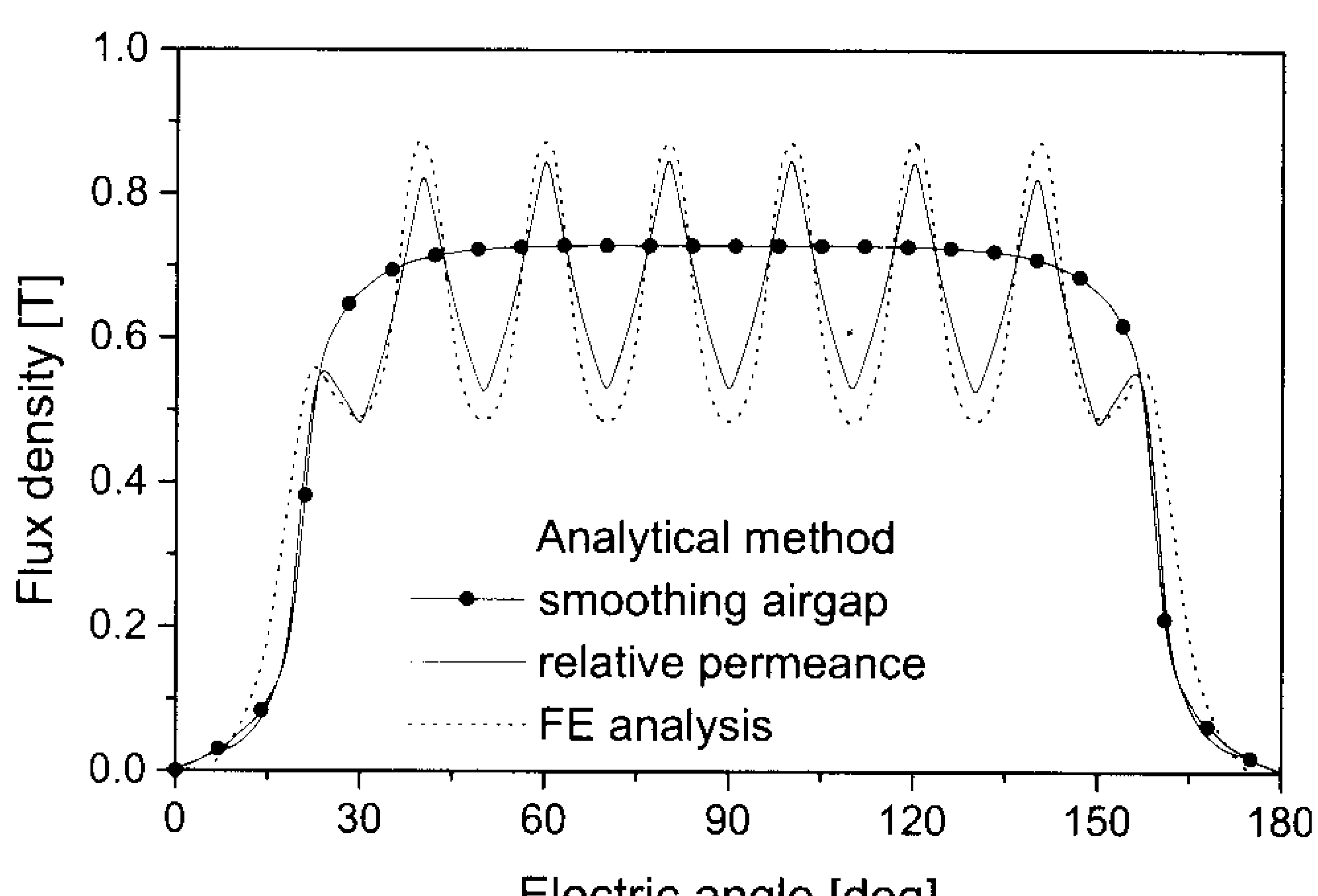

Fig. 5 Characteristic of airgap flux density (mechanical airgap center)

The magnetic field energy variations towards leading and trailing edges of the rotor poles can be significant as the rotor goes past the teeth and slots. The variations of magnetic field energy develop cogging torque and consequently the resultant torque pulsation is increased significantly [2]. Fig. 6 shows the Equi-potential distribution from FE analysis for calculating cogging torque then moving line technique is applied and the. cogging torque by using analytical method and 2-D FEM are shown in Fig. 7. The results of proposed method are in good agreement with 2-D FE analysis.

The IPMM generated by electro-magnetic torque and reluctancewhich is due to the difference of d-q axis inductance. Fig. 8 shows the components of torque in IPMM by the proposed analytical method and the comparison of the total torque including reluctance and cogging torque are shown in Fig. 9.

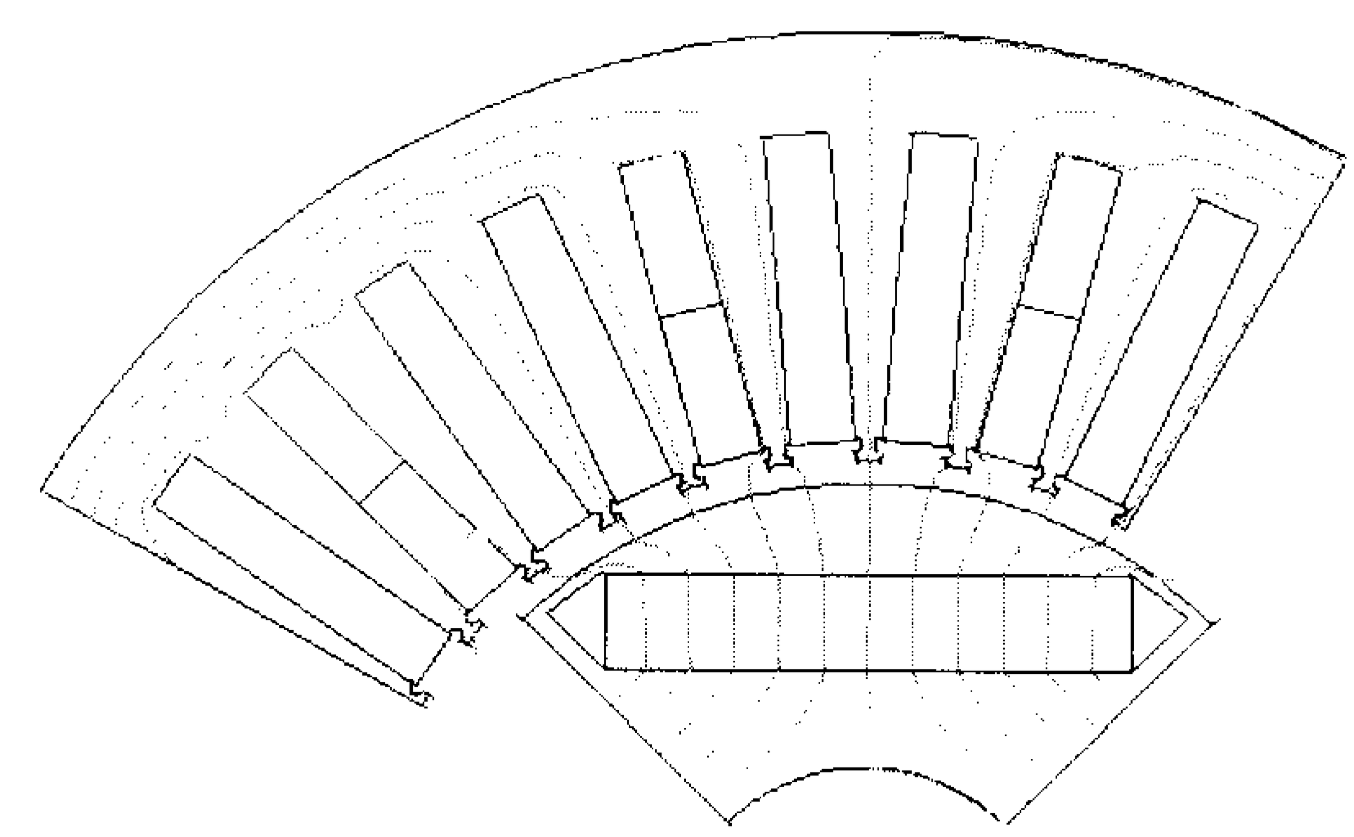

Fig. 6 Equi-potential distribution by moving line technique

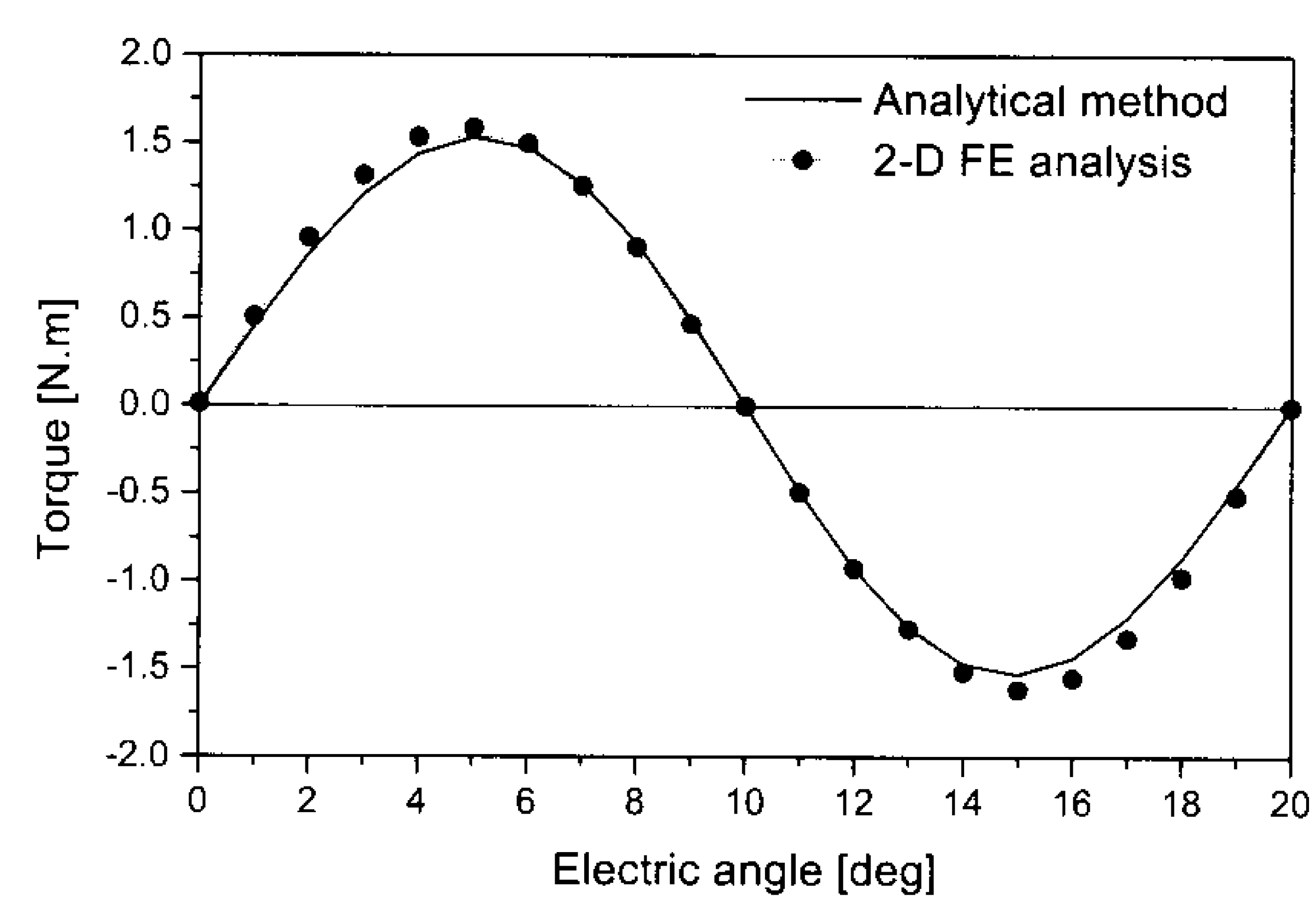

Fig. 7 Cogging torque characteristics of analysis model

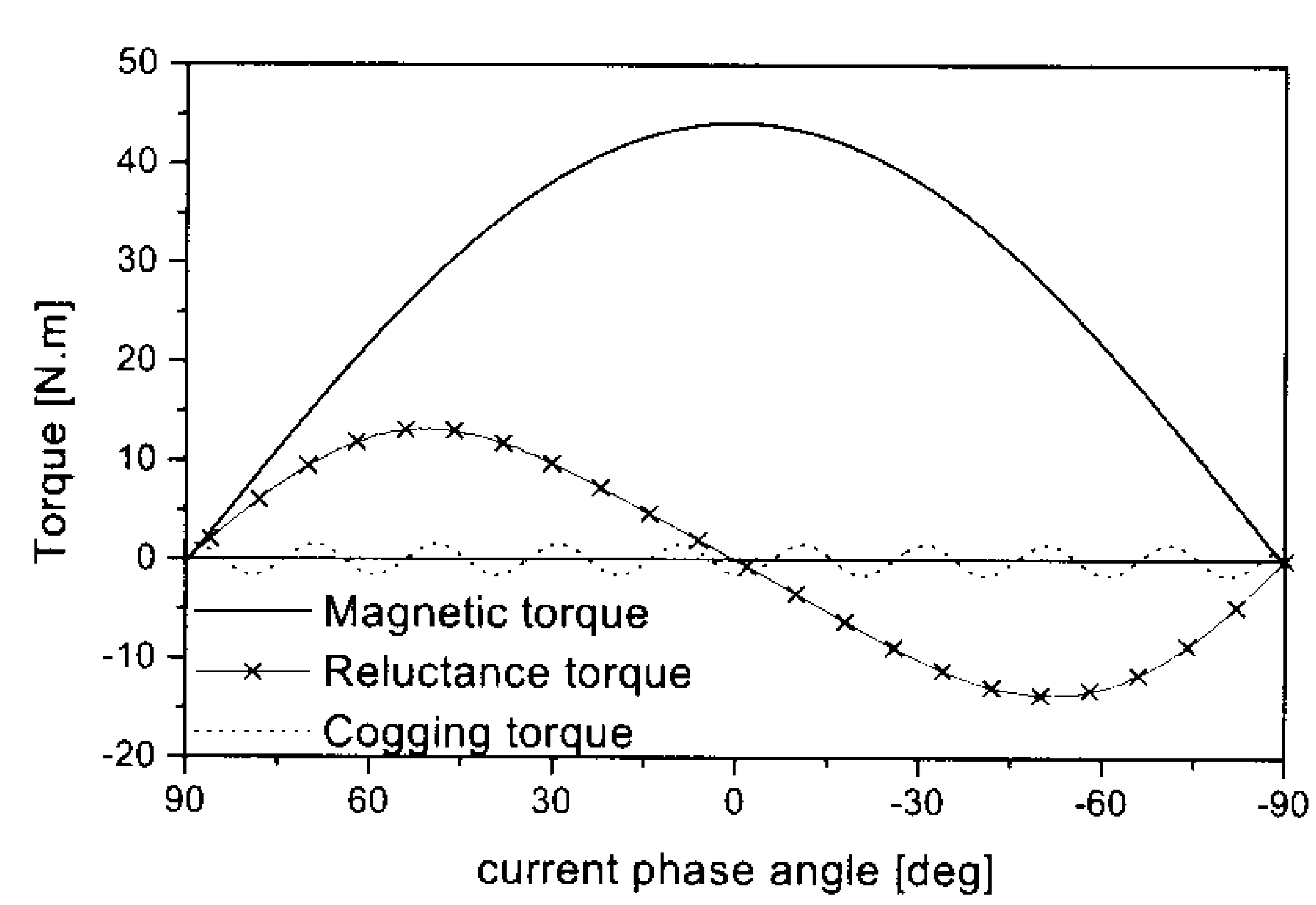

Fig. 8 Torque component by the analytical method

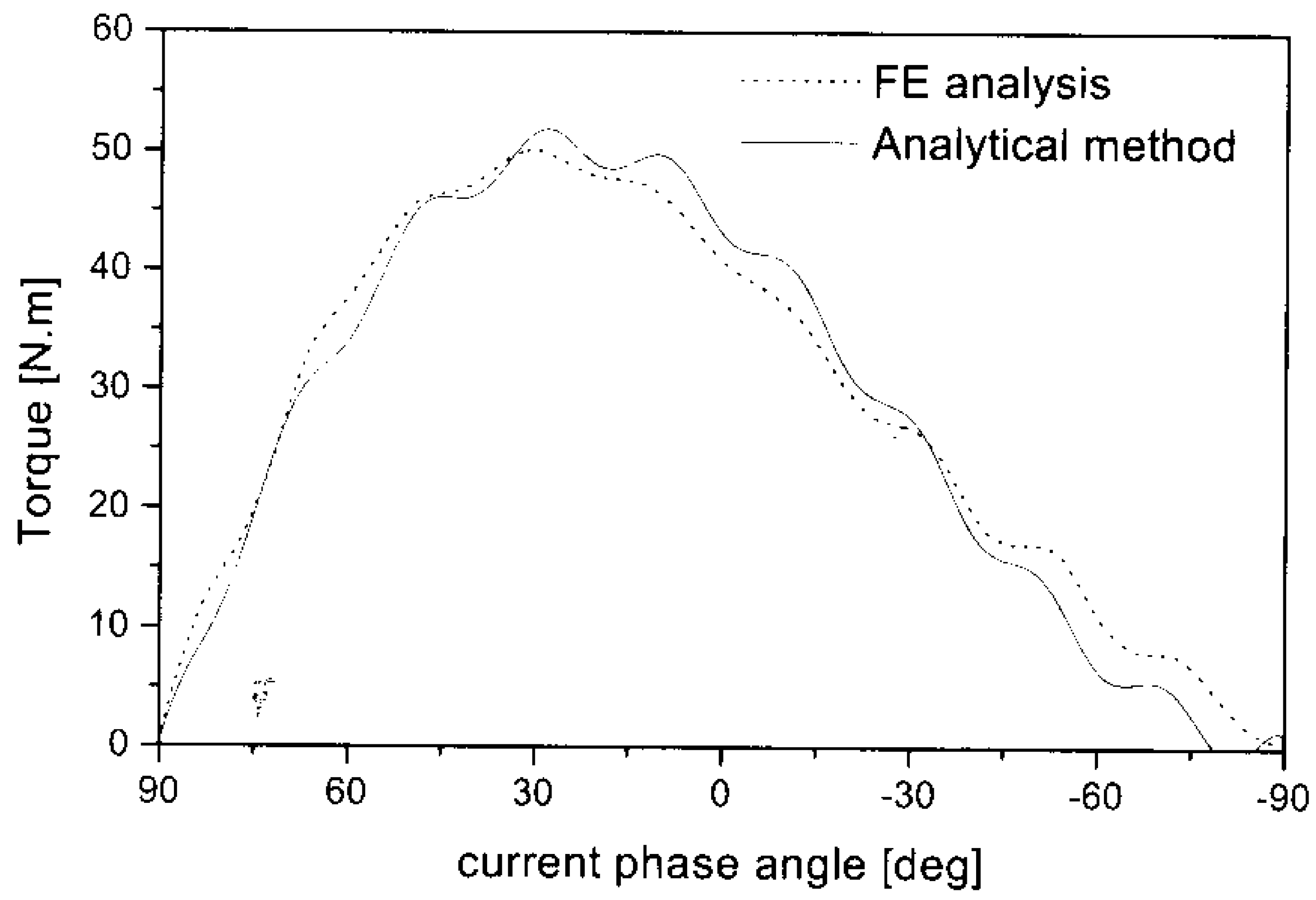

Fig. 9 Comparison of total torque

5. Minimization techniques of cogging torque

Cogging torque minimization techniques such as designing the air-gap length and slot opening width, shifting magnet poles and skewing either the stator teeth or magnet have been analyzed for various electromagnetic PM machines [7][8]. Skewing is the most common cogging torque minimization technique. Skewing reduces the harmonic content in the slots by uniformly distributing the magnetic field. With respect to cogging torque, similar results occur whether the stator or the rotor-mounted permanent magnets are skewed. In the case of buried PM machines, the methods of cogging torque reduction is presented by skewing the magnet and curvature of polar piece or varying the airgap length in one pole. It is prevent the sudden change of flux density levels at the rotor pole edges lead to significant cogging torque and improve the induced EMF waveform [2][7]. However, these increase the complexity and the constraint of the machine construction in IPMM. Therefore, in this paper, the reduction of cogging torque is achieved by changing the rotor shape while keeping the constant magnet dimension.

5.1 Inference of parameters on cogging torque

The cogging torque characteristics accordance with variation of design parameters are shown in Fig. 10~12. The cogging torque characteristics of IPMM are quite sensitive to the geometry of the rotor and the stator due to the small air-gap [2]. Fig. 10 shows the changing of cogging torque according to pole ratio and slot number combination. In slot to the number of 36, cogging torque is minimized at the pole ratio of 0.8. The characteristics of cogging torque by the changing of teeth width/slot open width is shown in Fig. 11 then slot is the number of 36. The larger ratio of teeth width/slot open width the less cogging torque is generated. Fig. 10, 11 shows that the cogging torque depends on not only the slot number and pole ratio combination but also teeth and slot width combination.

The characteristics of cogging torque by the changing of airgap length is shown in Fig. 12.

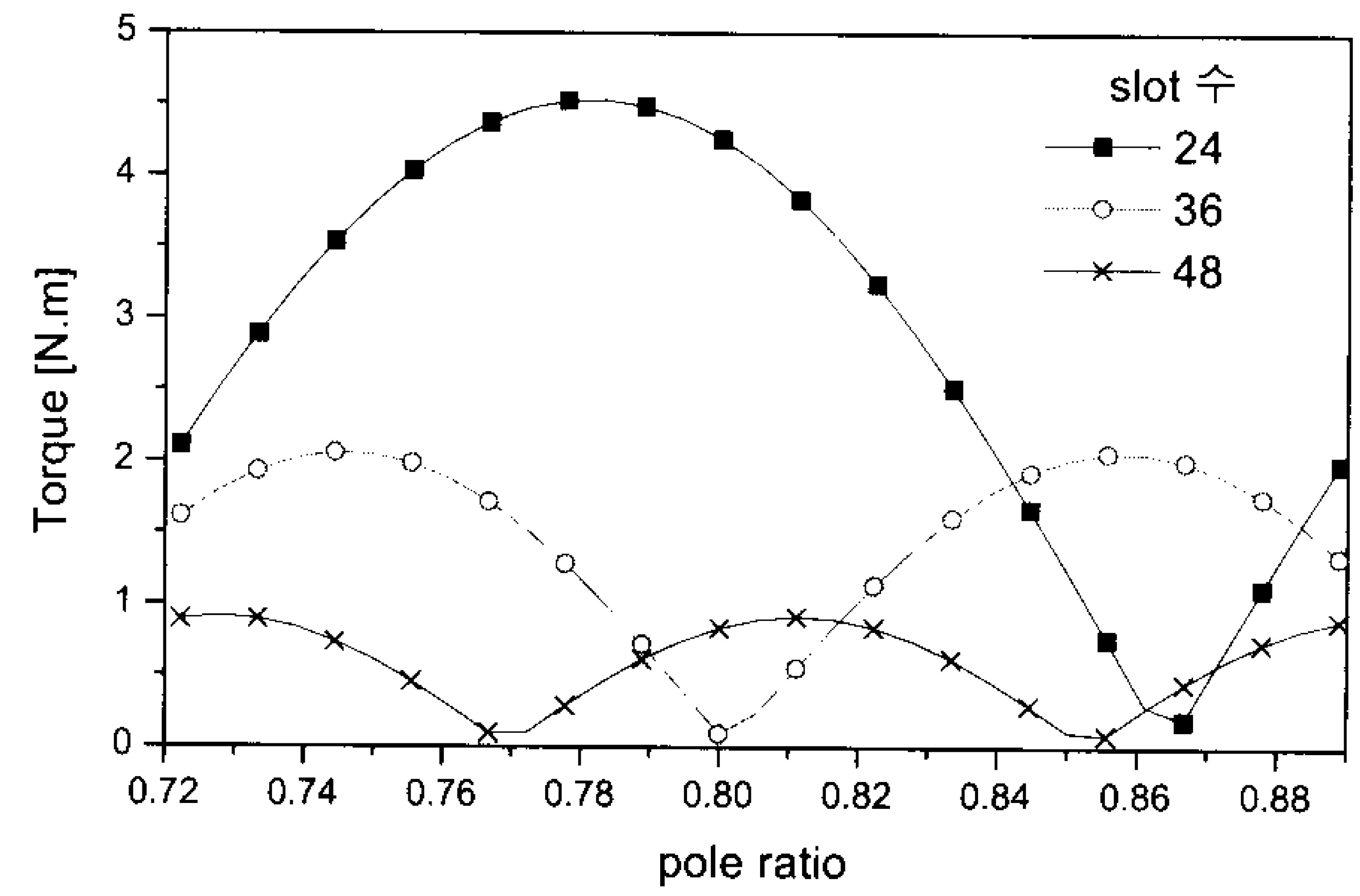

Fig. 10 Cogging torque characteristics according to pole ratio and slot number combination

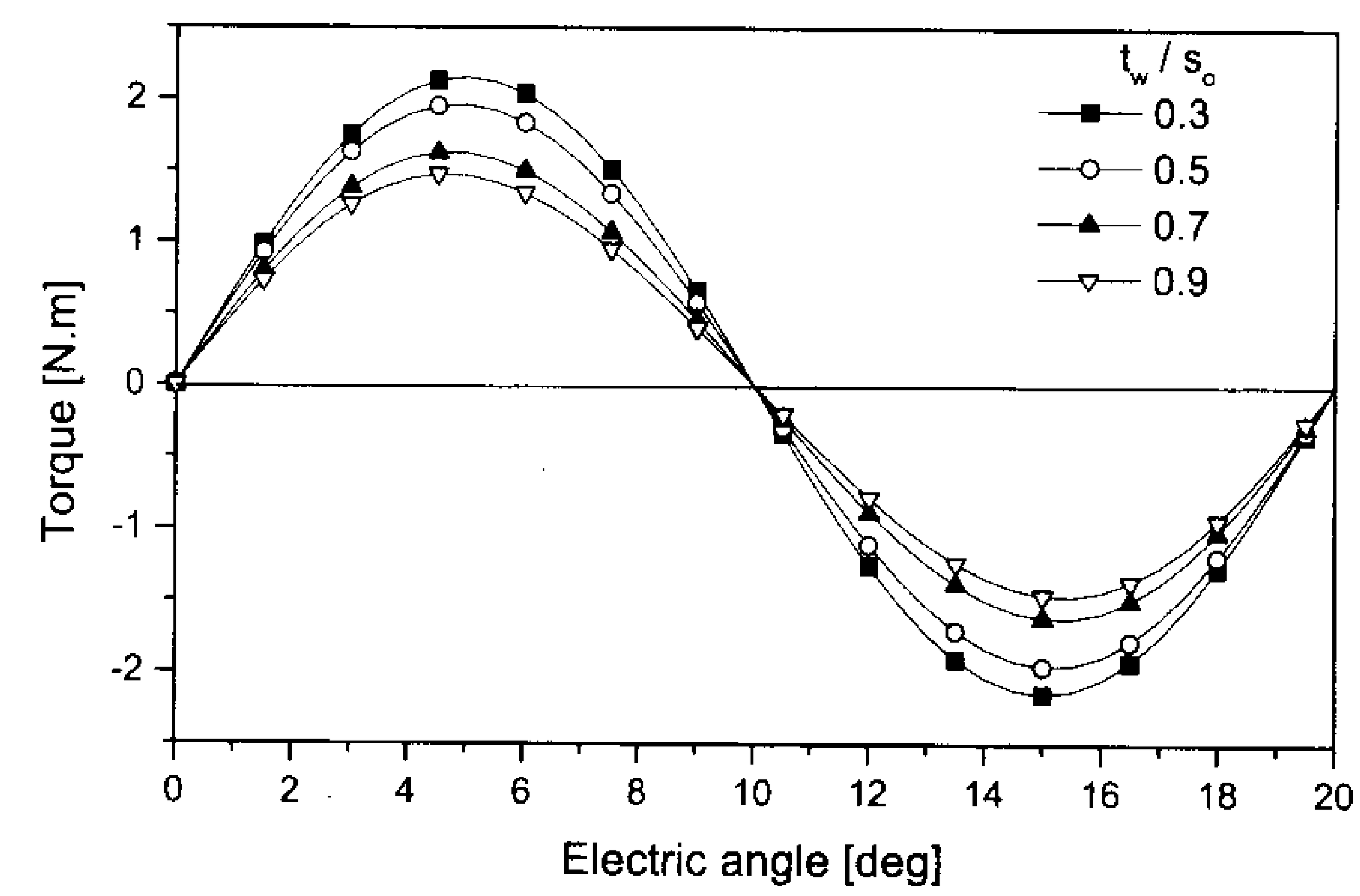

Fig. 11 Cogging torque characteristics according to teeth width / slot open width

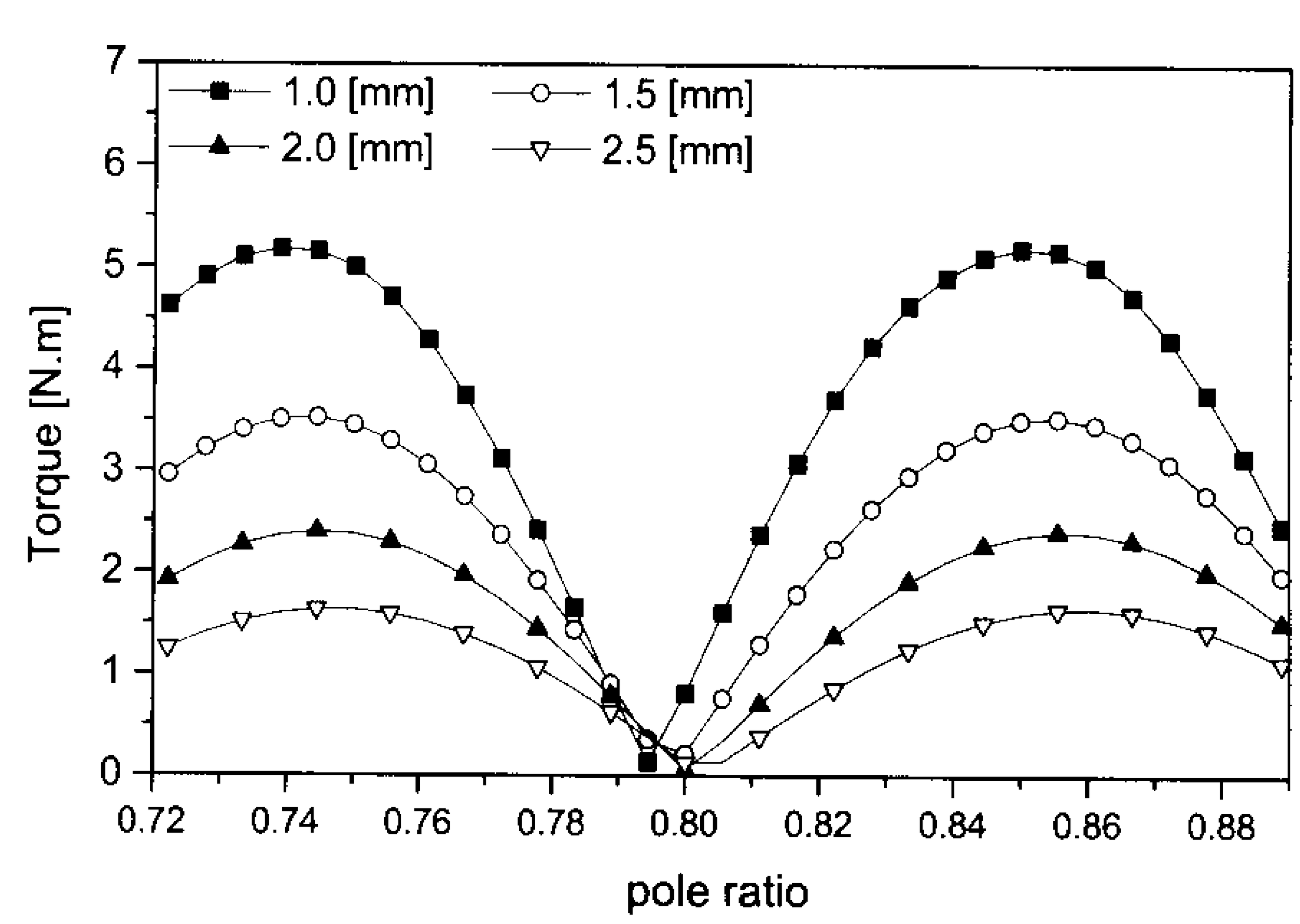

Fig. 12 Cogging torque characteristics according to airgap length

5.2 Shape design for reducing cogging torque

Certain design parameters can have a very significant effect on the cogging torque, in particular the pole ratio and slot number combination and skewing either the magnets or the teeth. However, skewing increase the complexity and the constraint of the machine construction in IPMM. In this study, the flux barrier angle is chosen as design parameter for minimization of cogging torque. The varying of flux barrier angle produces varying magnetic strength and magnet length, prevent the sudden change of flux density levels at the magnetic pole edges and can be some reducing the harmonics component of EMF. Above all, the realization is very easy. The design concept of rotor shape for varying the flux barrier angle is shown in Fig. 13.

The cogging torque is calculated from Maxwells stress tensor by using flux density in slots region that is calculated by relative permeance [5].

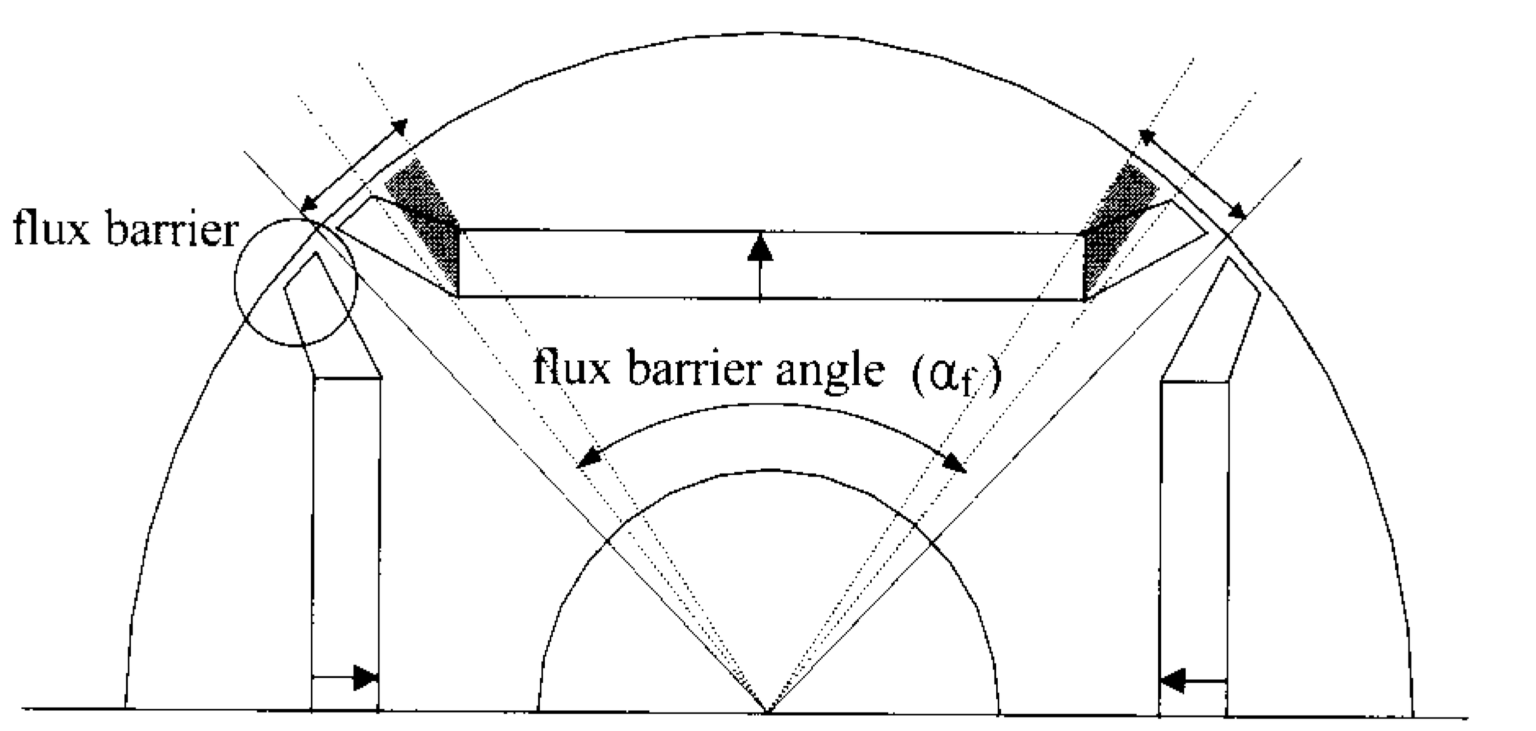

Fig. 13 Rotor shape design method for reducing cogging torque

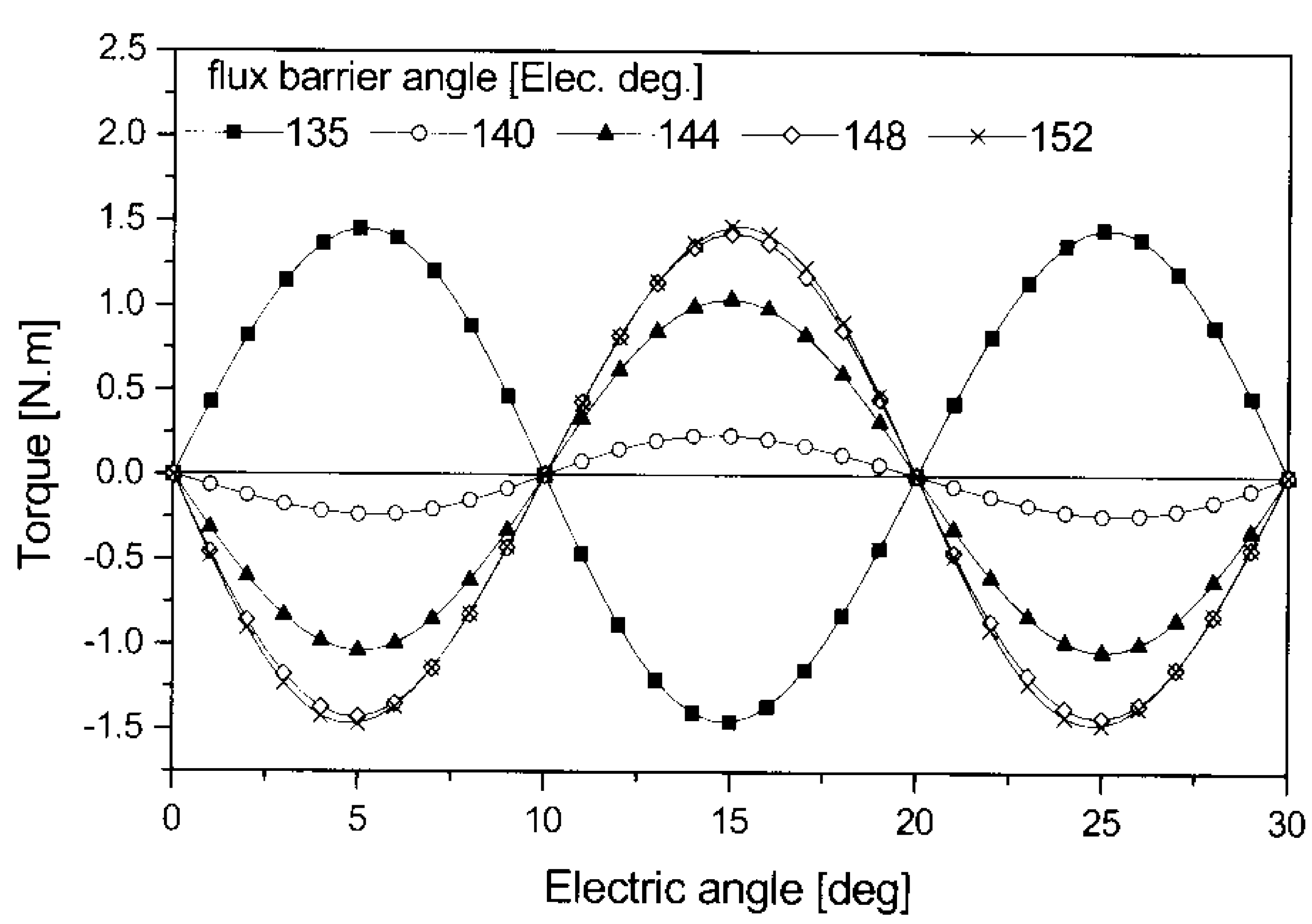

(a) cogging torque by proposed analytical method

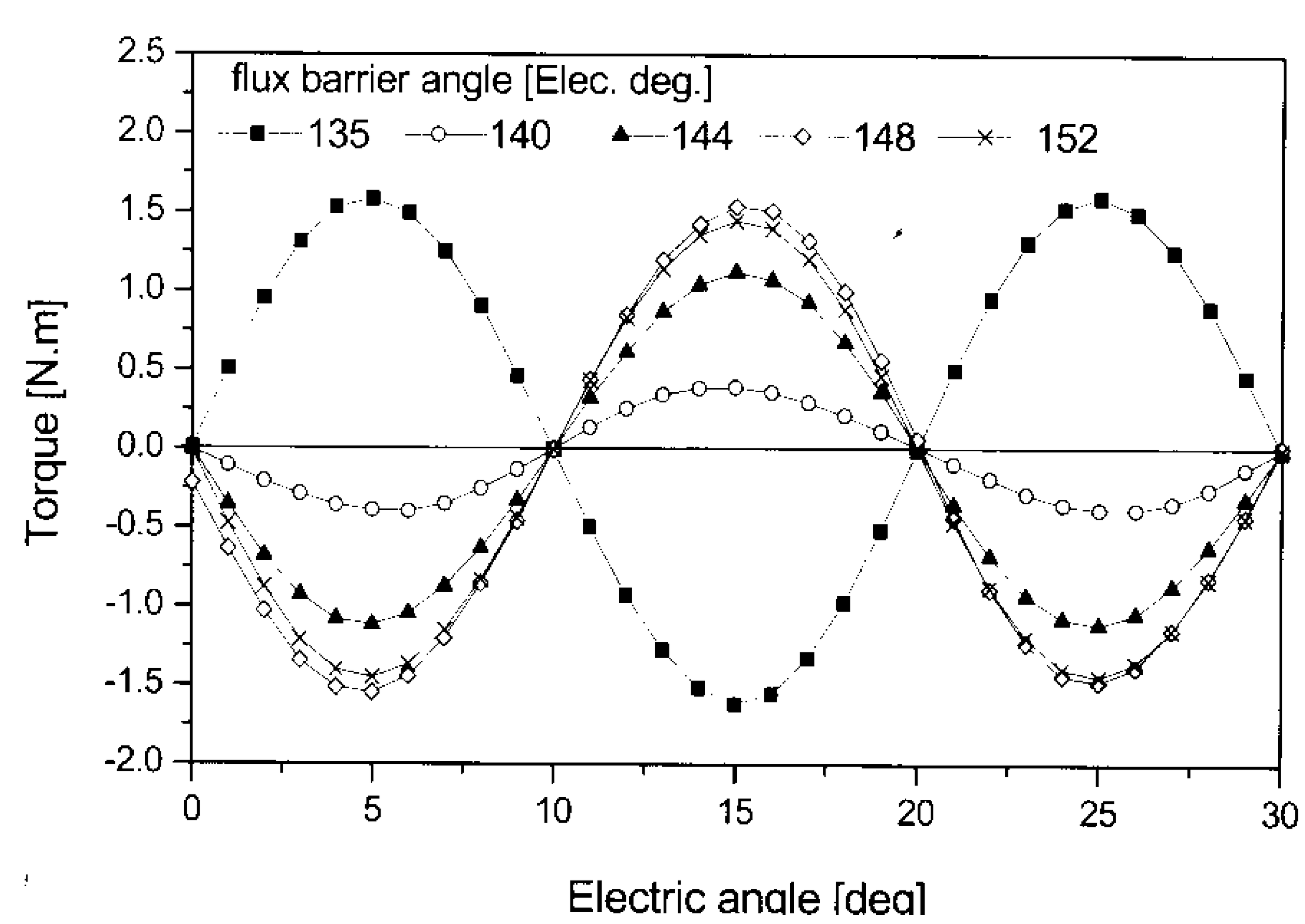

(b) cogging torque by FE analysis

Fig. 14 Cogging torque according to flux barrier angle

The cogging torque characteristics for different flux barrier angle are shown in Fig. 14. For the flux barrier angle of 140 (Elec.deg.), the peak value of cogging is minimized. It can be seen that the small variations of flux density distribution greatly affect on the cogging torque. The design results by analytical method are compared with 2-D FE analysis in Fig. 14(b). Results of the proposed design method for reducing the cogging torque are in good agreement compare with FE analysis.

The difference of d-q axis inductance is lead to reluctance torque. Fig. 15, 16 shows the d-q axis inductances according to flux barrier angle. As the variation of d-q axis inductance by the changing of flux barrier angle is generating hardly the reluctance torque is not almost change. Fig. 17 shows the total torque characteristics comparison initial model and improved model.

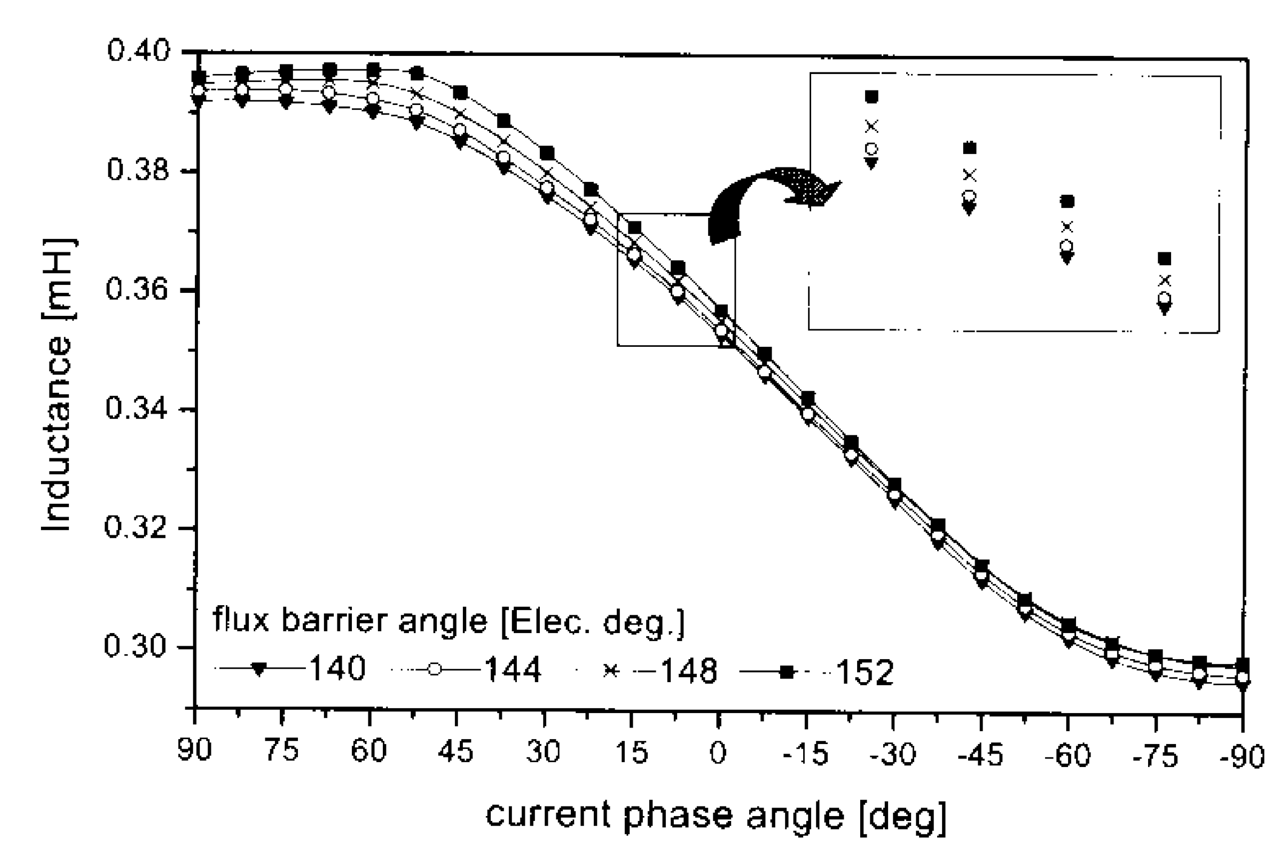

(a) d-axis inductances

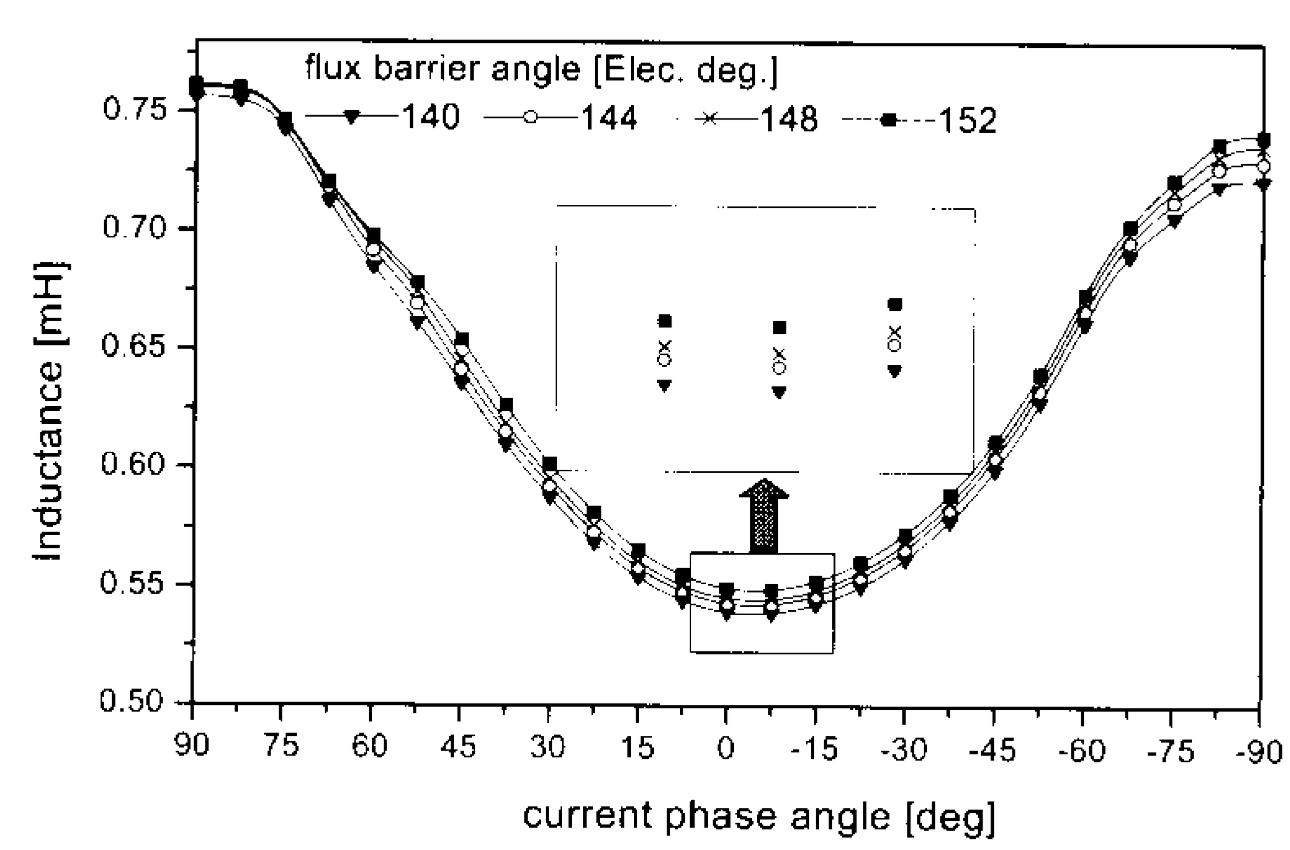

(b) q-axis inductance

Fig. 15 d-q axis inductance torque according to flux barrier angle

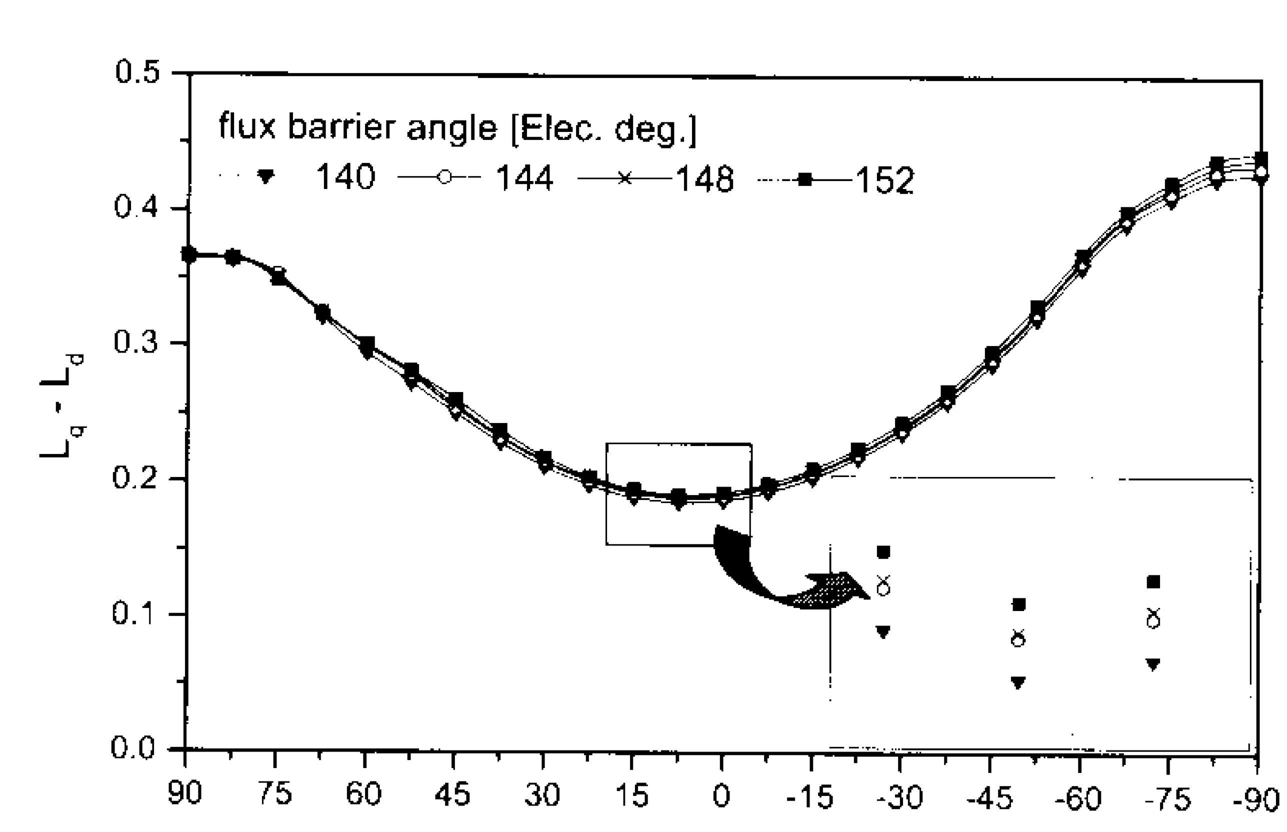

Fig. 16 Difference of d-q axis inductance according to flux barrier angle

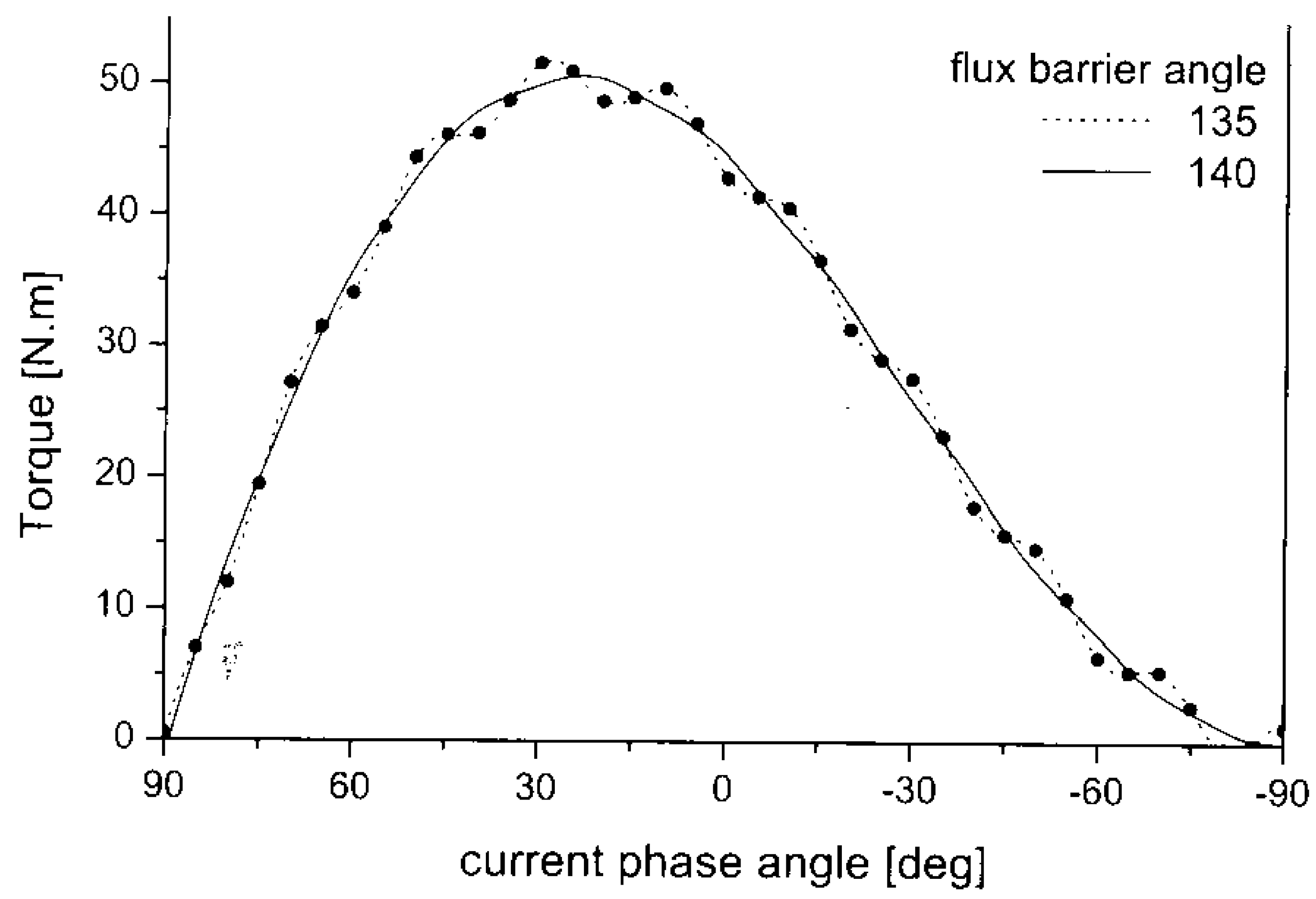

Fig. 17 Total torque characteristics according to flux barrier angle

6. Conclusions

The magnetic field and the cogging torque in the IPMM is calculated by the analytical method which is based on the spatial distribution of magnetization. In the case of IPMM, however, the actual pole ratio is different from the effective pole ratio. It is due to the leakage and fringing effect in link part that is working as flux barrier.

In this paper, we proposed an equivalent magnetizing distribution for leakage and fringing effect in flux barrier and the slotting effect is analyzed by coupling magnetic field analysis and relative permeance method. By using the analytical method, the new rotor shape is proposed to reduce the cogging torque under the constant magnet dimension without skewing. It is also found that the small variation of flux density distribution greatly affects the cogging torque. The results of the proposed analysis and shape design are verified against the 2-D FE analysis to give excellent aggreement..

To improve the accuracy in the computation and shape optimization for this system, the cogging torque should be analyzed by correct analytical method.

References

[1] E.Levi, "Saturation modelling in D-Q axis models of salient pole synchronous machines," *IEEE Transactions on Energy Conversion*, Vol. 14, No. 1, pp. 44-50, Mar. 1999

[2] E.R. Brage Filho, A.M.N. Lima and T.S. Araujo "Reducing cogging torque in interior permanent magnet machines without skewing", *IEEE Transactions on Magnetics*, vol. 34. no. 5, pp. 3652~3655, Sep. 1998

[3] Z.Q. Zhu, D. Howe, Ekkehard Bolte and Bernd Ackermann "Instantaneous magnetic field distribution in brushless permanent magnet dc motors, part I: open-circuit field" *IEEE Transactions on Magnetics*, vol. 29. no. 1. Jan 1993

[4] Ungtae Kim and Dennis K. Lieu "Magnetic field calculation in permanent magnet motors with rotor eccentricity: without slotting effect" IEEE Transactions on Magnetics, vol. 34. no. 4. July 1998

[5] Z.Q. Zhu and D. Howe "Analytical prediction of the cogging torque in radial-field permanent magnet brushless motors" *IEEE Transactions on Magnetics*, vol. 28. no. 2. March 1992

[6] Takeo Ishikawa and Gordon R. Slemon "A method of reducing ripple torque in permanent magnet motors without skewing" *IEEE Transactions on Magnetics*, vol. 29, no. 2, pp. 2028-2031, Mar.1997

[7] K.J. Binns, F.B.Chaaban and A.A.K. Hameed "Major design parameters of a solid canned permanent magnet motor with skewed magnets" IEE Proceeding-B, vol. 140, no. 3, pp. 161-165, May. 1993

[8] Jim-po Wang and Dennis K. Lieu "A fast lumped parameters for magnet skew in a motor", *IEEE Transactions on Magnetics*, vol. 35. no. 5, pp. 3709~3711, Sep. 1999

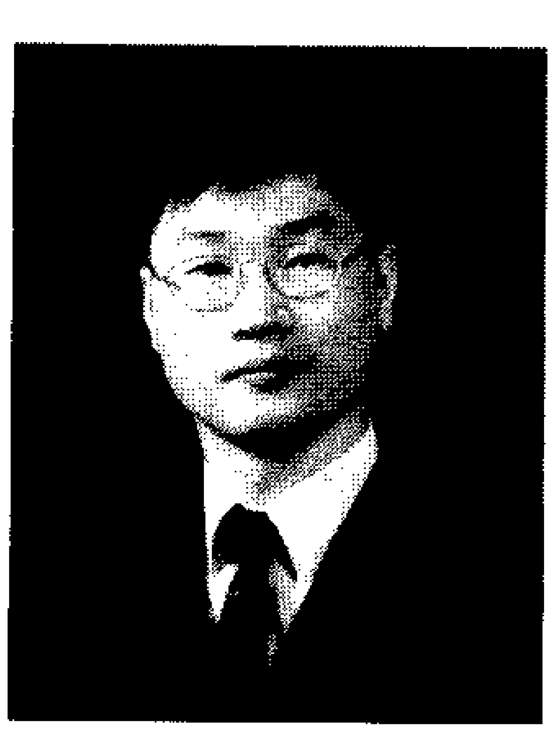

Gyu-Hong Kang was born in Korea in 1967. He received the B.E., M.E. and Ph.D. degrees from the Changwon National University, Changwon, Korea, in 1992, 1994 and 2001, respectively. He was with LG Electronics Inc. as Associate Research Engineer from 1994 to 1998. Since 2001, he has been B.K. Professor in the Department of Electrical Engineering at the Changwon National University, Changwon, Korea. His field of interest includes Design of Special Electrical Machine, Design of Servo Motor, Numerical Analysis of Electromagnetics.

Jung-Pyo Hong was born in Korea in 1959. He received B.Eng., M.Eng. and Ph.D.degrees from the Hanyang Univesity, Seoul, Korea. He was with LG Precision Co.,Ltd as Associate Research Engineer from 1990 and 1992, He joined Samsung Electric Co.,Ltd as Senior Research Engineer. Since 1996, he has been Lecturer in the Department of Electrical Engineering at the Changwon National University, Changwon, Korea. His field of interest includes Design of Special Electrical Machine, Design of Servo Motor, Numerical Analysis of Electromagnetics.

Gyu-Tak Kim was born in Korea in 1961. He received the B.Eng., M.Eng. and Ph.D.degrees from the Hanyang University, Seoul, Korea. Since 1991, he has been Lecturer in the Department of Electrical Engineering at the Changwon National University, Changwon, Korea. Between 1996 and 2001, he was a visiting researcher at Waseda University, Tokyo, Japan. His field of interest includes Numerical Analysis of Electromagnetics, Design of Electrical Machine, Special Electrical Machine, Energy Conversion Theory.